

# The matter content of the jet in M87: evidence for an electron-positron jet

C. S. Reynolds<sup>1</sup>, A. C. Fabian<sup>1</sup>, A. Celotti<sup>1,2</sup> and M. J. Rees<sup>1</sup>

<sup>1</sup>*Institute of Astronomy, Madingley Road, Cambridge CB3 0HA*

<sup>2</sup>*International School for Advanced Study, Trieste, Italy.*

## ABSTRACT

Recent observations have allowed the geometry and kinematics of the M87 jet to be tightly constrained. We combine these constraints with historical Very Long Baseline Interferometry (VLBI) results and the theory of synchrotron self-absorbed radio cores in order to investigate the physical properties of the jet. Our results strongly suggest the jet to be dominated by an electron-positron (pair) plasma. Although our conservative constraints cannot conclusively dismiss an electron-proton plasma, the viability of this solution is extremely vulnerable to further tightening of VLBI surface brightness limits. The arguments presented, coupled with future high-resolution multi-frequency VLBI studies of the jet core, will be able to firmly distinguish these two possibilities.

**Key words:** galaxies:jet - galaxies:individual:M87 - galaxies:active - elementary particles

## 1 INTRODUCTION

Jets are intimately linked with accretion processes. They can be found in almost all astrophysical situations in which matter is believed to be undergoing disk accretion onto some central collapsed object. Scales range from the slow ( $\sim 100 \text{ km s}^{-1}$ ) sub-parsec jets associated with forming stars to those found originating from powerful active galactic nuclei (AGN) which are initially relativistic and can propagate for hundreds of kpc before disrupting. Despite intense study, many basic questions remain open. The underlying formation mechanism is still uncertain (although hydromagnetic processes associated with the accretion disk seem a promising candidate mechanism: Blandford & Payne 1982; Lynden-Bell 1995 and references therein). Moreover, whereas jets from forming stars are believed to be molecular material entrained by a faster outflow of atomic material, the basic nature of AGN jets has not been unambiguously determined. Possibilities include an electron-proton plasma (i.e. normal material), an electron-positron plasma (i.e. a pair plasma), Poynting flux or combinations of these. This is an observationally difficult issue to address: even the handful of well studied jets only show power-law continuum radiation (presumably of synchrotron origin) with no sign of any spectral features from material moving with the bulk flow. This is to be contrasted with the Galactic source SS 433 in which the bulk flow of the jet is a known source of atomic line emission.

Celotti & Fabian (1993) have addressed the issue of the matter content of jets in a sample of radio-loud quasars and radio galaxies. Combining the synchrotron self-Compton

constraints with indications of the kinetic luminosity suggest that, for the sample as a whole, the jets are either cold electron-positron flows or electron-proton flows with an electron low-energy cutoff of  $\sim 50 \text{ MeV}$ . They argue for the electron-proton case on the basis of annihilation constraints under the assumption that the pairs originate from the inner regions of the accretion flow. However, the issue of the matter content of any one given extragalactic jet (as opposed to a large, possibly heterogeneous, sample) has not been addressed in detail. An (observationally based) determination of the matter content of an individual well studied jet would be an important step in the study of jet formation, propagation and emission.

M87 (NGC 4486) is a giant elliptical galaxy near the centre of the Virgo cluster of galaxies. It is associated with the radio source (Virgo-A, 3C 274) and classified as a FR-I radio galaxy (Fanaroff & Riley 1974) on the basis of its edge-darkened morphology and low radio luminosity ( $P_{178\text{MHz}} \sim 1 \times 10^{32} \text{ erg s}^{-1} \text{ Hz}^{-1}$ ). This galaxy contains the most spectacular example of an extragalactic jet in the northern sky. It was the first extragalactic jet to be discovered (Curtis 1918) and, since then, it has been subjected to intense observational studies at all wavelengths (see Biretta 1993 for a recent review). The complex knotty structure of the jet has been resolved at wavelengths from the radio through to X-rays (Biretta, Stern & Harris 1991). The spectrum and proper motions (Biretta, Zhou & Owen 1995) of the knots yield direct constraints on the physical processes operating and the geometry of the system. Hubble Space Telescope (HST) studies of the base of the jet reveal a rotating gas disk apparently lying normal to the jet direction (Ford et al.

1994; Harms et al. 1994). The projected appearance and velocity of the disk suggests it to be at an inclination of  $42 \pm 5^\circ$  and to enclose a mass of  $(2.4 \pm 0.7) \times 10^9 M_\odot$ . Also, Very Long Baseline Interferometry (VLBI) has resolved structure within the core of M87 on spatial scales of  $\sim 0.01$  pc. The VLBI studies will be discussed in more detail in Section 3.1. The synchrotron spectrum of this jet has been recently examined by Meisenheimer, Röser & Schlötelburg (1996). This wealth of data makes M87 the most promising candidate for any physical study of extragalactic jets.

In this paper we combine these observational constraints of the M87 jet with the theory of synchrotron radiation in order to constrain the physical parameters of the jet. In particular, we address the particle density, magnetic flux density and the matter content of the jet. In order to keep this paper focussed, our treatment is as model independent as possible. The arguments we use depend only upon an observationally well determined kinematic model and the standard synchrotron jet model of Blandford & Königl (1979). Our arguments are independent of any models (of which there are a plethora) for the initial formation, collimation and acceleration of the jet. Section 2 briefly reviews the relevant observations and the kinematic model to which they lead (Biretta 1993; Biretta, Zhou & Owen 1995). Section 3 discusses the synchrotron self-absorption model for the radio emission from the core and the subsequent constraints on the particle density and the magnetic flux density. Section 4 places further constraints on the particle density of the jet using the large scale limits on the total kinetic luminosity. The resulting constraints suggest the jet to be electron-positron dominated rather than electron-proton dominated. Section 5 discusses the robustness of the result and some implications. It is found that an electron-proton jet possessing an electron population with a low-energy cutoff  $\sim 10m_e c^2$  also satisfies our constraints although this solution is extremely vulnerable to further tightening of the VLBI surface brightness lower limit. Section 6 summarizes our conclusions.

Stellar surface brightness fluctuations give a distance to M87 of  $15.9 \pm 0.9$  Mpc (Tonry 1991), independently of Hubble's constant. In the rest of this paper we assume a distance to M87 of 16 Mpc.

## 2 KINEMATIC MODEL

In this work, we use the kinematic model for the M87 jet presented in Biretta (1993; hereafter B93) and Biretta, Zhou & Owen (1995; hereafter BZO). This is based on detailed observations of proper motions within the knotty structure of the jet. In this model, the inner jet is relativistic with a bulk flow Lorentz factor,  $\Gamma \gtrsim 3$ . The prominent knot A marks the location of a strong relativistic shock in which the flow slows from velocities of  $\sim c$  to  $c/3$  (in the frame of reference in which the shock is stationary). In the observers frame, the Lorentz factor decreases across the shock from  $\Gamma \sim 3$  to  $\Gamma \sim 1.5$ . The flow suffers another shock at knot C at which it is decelerated to subrelativistic velocities. The jet then disrupts and merges into the radio halo. The orientation of the jet axis to the line of sight,  $\theta$ , is between  $30\text{--}40^\circ$ .

The relatively large angle to the line of sight ( $30\text{--}40^\circ$ )

puts severe limits on the extent to which relativistic beaming can be important. This fact will be extensively used in the later sections. The effects of beaming are characterized by the *beaming parameter*,  $\delta$ , defined by

$$\delta = \frac{1}{\Gamma(1 - \beta \cos\theta)}, \quad (1)$$

where  $\beta c$  is the bulk velocity of the material in the observers frame. For a given  $\theta$ , this has a maximum value of

$$\delta_{\max} = \frac{1}{\sin\theta}, \quad (2)$$

corresponding to  $\beta = \cos\theta$ . Evaluating for  $\theta = 30^\circ$  gives  $\delta_{\max} = 2$  (and increasing  $\theta$  will result in decreasing  $\delta_{\max}$ ). Thus, relativistic effects can only produce a moderate increase in the observed luminosity of features moving along the jet. Moreover, for  $\Gamma \gtrsim 7$  (given  $\theta = 30^\circ$ ) relativistic aberration diminishes the observed luminosity since it is beamed away from the observer.

We note that relativistic beaming is important in rendering the counter-jet undetectable. Assuming the system to contain two intrinsically symmetric (back-to-back) jets, a bulk Lorentz factor of  $\Gamma \gtrsim 3$  and  $\theta = 30^\circ$  results in a jet/counter-jet flux ratio of  $\gtrsim 300$ . The observational limits on the jet/counter-jet (radio) flux ratio (based on the non-detection of the counter-jet) are  $\sim 150$  (Biretta 1993).

## 3 SYNCHROTRON SELF-ABSORPTION CONSTRAINTS

### 3.1 Basic model for the core emission

Like many extragalactic radio sources, the core of M87 has a flat radio spectrum (see Fig. 5 of Biretta, Stern & Harris 1991; hereafter BSH). This is generally believed to be due to the superposition of many synchrotron emitting components, each of which has a different self-absorption frequency (Blandford & Königl 1979). In the diverging flow of the inner jet, these components correspond to emitting regions at different distances along the jet. The observed flux density at a given frequency is then dominated by the region of the jet which becomes self-absorbed at that (Doppler shifted) frequency.

Consider one such region of the jet which is just becoming self-absorbed at the jet rest-frame frequency  $\nu'_m$ . Radiation with this frequency will suffer relativistic Doppler shifts to an observer-frame frequency  $\nu_m = \nu'_m \delta$ . Suppose the corresponding flux density from the self absorbed region in the observers frame is  $F_m$ . Observations of the core at the frequency  $\nu_m$  will measure this flux density plus contributions from optically thin parts of the jet. The total observed core flux density at  $\nu_m$  will be  $F_{\text{tot}}(\nu_m) = \eta F_m$  where  $\eta > 1$  allows for the emission from the optically thin parts of the jet. Within the flat spectrum regime, most of the emission must be dominated by the self-absorbed region of the jet: thus we impose the condition that  $\eta \lesssim 2$ . If the observations also resolve the flat spectrum core, the resulting dimension is a measure of the diameter of the jet at the self-absorption point.

VLBI observations of M87 have been performed at a number of frequencies. Reid et al. (1989) present 1.66 GHz

VLBI observations of the nuclear region of M87 showing a well collimated knotty jet extending from an unresolved core. These observations also show subluminal motion within these knots suggesting that the pattern speed is very much slower than the fluid speed. The 5 GHz observations of Pauliny-Toth et al. (1981) just resolve the core to have a (major axis) angular diameter of  $\theta_d = 0.7$  mas (corresponding to 0.06 pc at the distance of M87) and a total core flux of  $F_m = 1.0$  Jy. Higher frequency observations probe deeper into the core of the jet before encountering the self-absorption surface as well as achieving a better angular resolution. Thus, 22 GHz VLBI observations with a resolution of  $\sim 0.15$  mas (corresponding to 0.01 pc; Spencer & Junor 1986; Junor & Biretta 1995) reveal an unresolved core (peak surface brightness  $0.34$  Jy beam $^{-1}$ ) and a stationary pattern of knots stretching for 4 mas in the approximate direction of the large scale jet. The best resolution has been achieved with 100 GHz VLBI (Bääh et al. 1992) which reveals several unresolved knots within 0.1 mas of the core. The flat spectrum nature of the core is consistent with it being self absorbed up to frequencies of at least 22 GHz and possibly even 100 GHz (Spencer, private communication).

In the remainder of this section, we use the 5 GHz VLBI constraints on the flux and dimensions of the self-absorbed region to place constraints on the relativistic (synchrotron emitting) proper particle density,  $n$ , and magnetic flux density,  $B$ , at this location within the jet. We assume a uniform jet in the sense that  $n$ ,  $B$  and  $\beta$  are constant across cross-sections of the jet.

### 3.2 Surface brightness of the self-absorbed region

Here we follow the work of Ghisellini et al. (1992; hereafter G92). Suppose the relativistic electrons responsible for the synchrotron radiation have a differential Lorentz-factor distribution of  $N(\gamma) = N_0 \gamma^{-(2\alpha+1)}$  for  $\gamma_{\min} < \gamma < \gamma_{\max}$  where  $\gamma$  is the electron Lorentz factor as measured in the rest frame of the jet material.

In the optically-thin regime (and well away from the low-frequency or high-frequency cutoff), this produces synchrotron emission with a spectral index  $\alpha$ . For the M87 jet,  $\alpha \sim 0.5$ . The proper relativistic particle number density is given by

$$n = \int_{\gamma_{\min}}^{\gamma_{\max}} N(\gamma) d\gamma. \quad (3)$$

For  $\alpha > 0$  and  $\gamma_{\max} \gg \gamma_{\min}$ , this integral is dominated by the value of  $\gamma_{\min}$ . The particle number density,  $n$ , is then related to the normalization of the relativistic electron distribution,  $N_0$ , by

$$N_0 = 2\alpha \gamma_{\min}^{2\alpha} n = \gamma_{\min} n, \quad (4)$$

where we have used  $\alpha = 0.5$  in order to obtain the last expression. In this case the mean Lorentz factor of an electron is given by

$$\langle \gamma \rangle = \gamma_{\min} \ln \left( \frac{\gamma_{\max}}{\gamma_{\min}} \right). \quad (5)$$

For  $\gamma_{\min} = 1$ , any reasonable choice of  $\gamma_{\max}$  gives  $\langle \gamma \rangle \sim 10$ .

The synchrotron flux in the self-absorbed regime is independent of particle density. Thus, our constraints on  $F_m$

and  $\theta_d$  can be translated into a constraint on  $B$ . In particular, there is a relationship between  $B$  and the surface brightness of the self-absorbed region (e.g. see G92) which gives,

$$B \lesssim 10^{-5} b(\alpha) \theta_d^4 F_m^{-2} \nu_m^5 \frac{\delta_{\max}}{1+z} \text{ G}, \quad (6)$$

where  $\theta_d$  is in milliarcsec,  $F_m$  is in Jy and  $b(\alpha)$  is a function tabulated in G92. The inequality results from the limit on  $\delta$ . From G92,  $b(\alpha = 0.5) \approx 3.2$ , and noting that  $\delta_{\max} \approx 2$  gives  $B < 0.2$  G. This constraint is plotted on Fig. 1 (shaded areas represent forbidden regions within the  $n, B$  plane.)

### 3.3 Optical depth of the self-absorbed region

The point at which the jet is just becoming self-absorbed at an observed frequency  $\nu_m$  is defined by  $\kappa(\nu_m)X = 1$  where  $\kappa(\nu)$  is the absorption coefficient for synchrotron absorption at frequency  $\nu$  and  $X$  is the path length of the line of sight through the jet. Using the standard result for the rest-frame absorption coefficient (Jones, O'Dell & Stein 1974; Rybicki & Lightman 1979) and noting that  $\nu_m = \nu'_m \delta$  gives

$$\kappa(\nu_m) = \frac{3^{\alpha+1} \pi^{1/2} g(p) e^2 N_0}{8 m_e c} \nu_B^{-(3/2+\alpha)} \nu_m^{-(5/2+\alpha)} \delta^{(5/2+\alpha)}, \quad (7)$$

(cgs units) where  $\nu_B$  is the cyclotron frequency,  $p = 2\alpha + 1$  and  $g(p)$  is the given in terms of Gamma functions by

$$g(p) = \frac{\Gamma((3p+22)/12) \Gamma((3p+2)/12) \Gamma((p+6)/4)}{\Gamma((p+8)/4)} \quad (8)$$

This expression for  $\kappa(\nu)$  is valid for  $\nu \gg \nu_{\min} \approx \gamma_{\min}^2 \nu_B$ , where  $\nu_{\min}$  is the low-energy cutoff in the synchrotron spectrum corresponding to the low-energy cutoff in the electron energy distribution. In this regime the self-absorption depends only on the normalization of the relativistic electron energy distribution and not on details of the low-energy cutoff. The spectrum of BSH shows no evidence for such a low-energy cutoff thereby giving us confidence that the observed frequencies lie in the domain of applicability of eqn (7).

We also need to relate the observer-frame line of sight path length through the jet,  $X$ , with the physical jet diameter,  $2r$ . Taking into the account the relativistic transformations, the required relation (for a cylindrical geometry) is

$$X = \frac{2r}{\delta \sin \theta}. \quad (9)$$

Evaluating the above condition on the optical depth for  $\alpha = 0.5$  gives  $nB^2 > 2\gamma_{\min}^{-1} \delta_{\max}^{-2}$  (cgs). For the moment we assume that  $\gamma_{\min} = 1$  (i.e. that the electron energy distribution extends down to non-relativistic energies). Relaxation of this assumption will be discussed in Section 5.3. The assumed geometry implies  $\delta \lesssim 2$  leading to  $nB^2 \gtrsim 0.5$  (cgs). This is our second constraint on the  $n, B$  plane (Fig. 1).

## 4 KINETIC LUMINOSITY CONSTRAINTS

The total kinetic luminosity of the jet is an important observational parameter. In this section we estimate the total (time-averaged) kinetic power of the jet by examining the energetics of the system as a whole. We then assume the

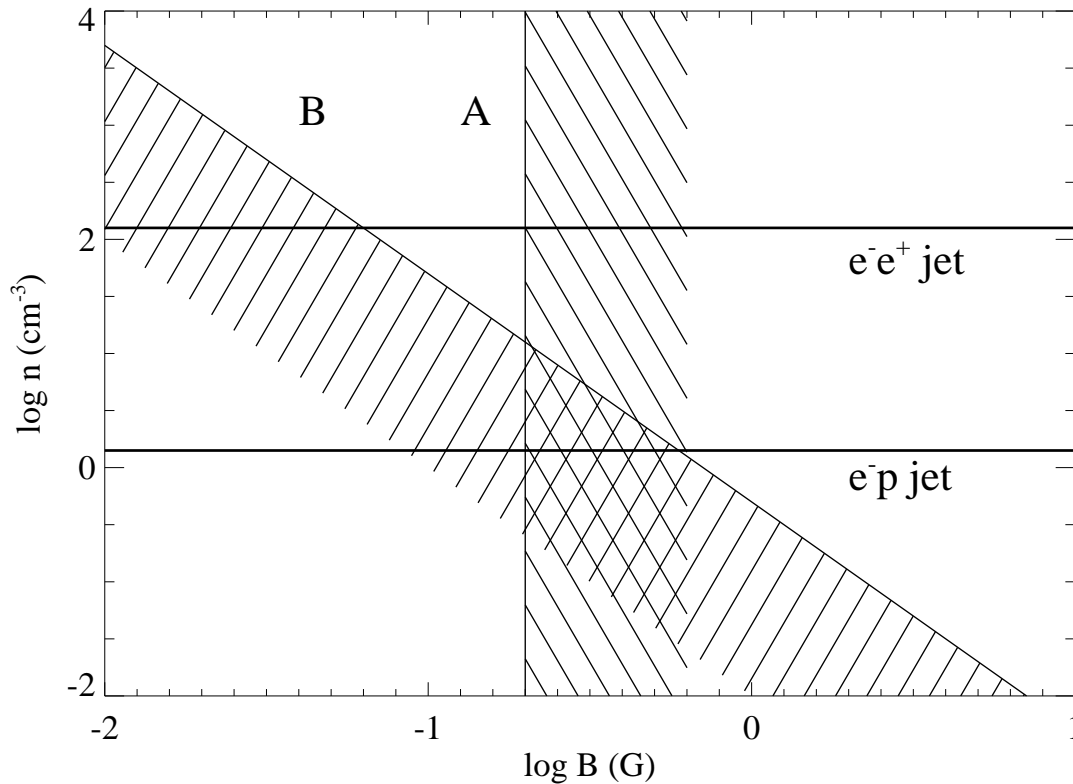


**Figure 1.** Constraints on the  $B$ - $n$  plane imposed by synchrotron self-absorption and total kinetic luminosity considerations. The 5 GHz VLBI surface brightness constraint on  $B$  gives line A. Line B corresponds to the condition that resolved core of the jet is just becoming optically thick to self-absorption. The horizontal lines are the densities derived by imposing  $L_{43} = 1$  for the two cases of a pair jet (with  $\gamma_{\min} = 1$  and  $\langle \gamma \rangle \approx 10$ ) and a cold jet of normal matter.

VLBI jet carries this same kinetic power in order to place independent constraints on its properties.

#### 4.1 The global energy balance

Ultimately, the kinetic energy carried by the jet can be radiated (at the knots, for example), can perform work on the surrounding interstellar medium (ISM) to expand the radio halo or can be stored in relativistic particles within the radio halo. Here we assess the kinetic luminosity of the jet by summing these components.

##### 4.1.1 Radiated energy

A multiwaveband study of the radiant emissions from the jet has been performed by BSH. By summing the observed emission of the jet (dominated by emission from knots A and B) as tabulated in BSH, we estimate that  $\sim 3 \times 10^{42}$  erg s $^{-1}$  is radiated along the length of the jet. As stated above, relativistic beaming will not have a major effect on the observed luminosity.

##### 4.1.2 Energy stored within the radio halo

The large scale radio morphology of the system (Turland 1975) suggests the presence of an inner radio halo ( $\sim 5$  kpc

in extent) embedded in a larger, more diffuse, halo ( $\sim 50$  kpc in extent). The inner structure is clearly associated with the current phase of nuclear activity since the jet can be observationally traced from its origins in the nucleus to the point at which it disrupts and feeds this radio halo (e.g. see VLA images of Owen, Hardee & Bignell 1980 and, more recently, Hines, Owen & Eilek 1989). Spectral curvature arguments suggest an age of  $\sim 10^6$  yr for this inner structure. The extensive outer halo is probably associated with a previous phase of activity and will not be considered further here.

Estimating the energy stored within the inner radio halo amounts to determining the pressure of this structure. Radio observations allow the minimum (i.e. equipartition) pressure  $p_{\min}$  of the synchrotron emitting plasma to be determined. The VLA data presented by Hines, Owen & Eilek (1989) show the inner radio lobe to have a filamentary structure with the minimum pressure of the average filament being  $p_{\min} \sim 2\text{--}6 \times 10^{-10}$  dyn cm $^{-2}$ . The brightest filaments have  $p_{\min} \sim 10^{-9}$  dyn cm $^{-2}$  whereas the interfilamentary plasma has  $p_{\min} \sim 4 \times 10^{-11}$  dyn cm $^{-2}$ . X-ray observations of thermal emission from the interstellar medium (ISM) also allow the ISM pressure to be determined at the vicinity where it comes into contact with the inner radio halo. A deprojection analysis (Fabian et al. 1981) of data from the *ROSAT* high-resolution imager (HRI) reveals an ISM pressure of  $p_X \approx 5 \times 10^{-10}$  dyn cm $^{-2}$  (C. B. Peres, private communica-

tion). Thus the highest minimum pressures obtained from radio observations exceed the ISM pressure by a factor of 2. The amount by which the radio halo is overpressured with respect to the ISM can be estimated by considering the expansion of an overpressured bubble. Bicknell & Begelman (1996) present such a model for the M87 system and show that the inner radio halo should be overpressured with respect to the ISM by a factor of  $\sim 3$ . Independent support for this mild overpressure comes from the observed optical emission line filaments discovered by Ford & Butcher (1979) and studied in greater detail by Sparks, Ford and Kinney (1993). Bicknell & Begelman (1996) show how the expansion of this mildly overpressured halo energizes the optical emission line filaments.

To conclude this argument, the pressure of the inner radio halo is likely to be  $p \approx 1.5 \times 10^{-9} \text{ dyn cm}^{-2}$ , leading to a stored energy within the halo of  $6 \times 10^{56} \text{ erg}$ . The total kinetic luminosity required to supply this energy in  $10^6 \text{ yr}$  is  $2 \times 10^{43} \text{ erg s}^{-1}$ . If there is a symmetric counter jet (as assumed in the classic twin-jet model), the single-jet kinetic luminosity which contributes to the relativistic particle energy in the halo is  $1 \times 10^{43} \text{ erg s}^{-1}$ .

#### 4.1.3 Time-averaged kinetic luminosity, $L_K$

Summing the above contributions, the kinetic luminosity of the jet (averaged over the duration of the current period of activity) is  $L_K = 10^{43} L_{43} \text{ erg s}^{-1}$  where  $L_{43} \sim 1$ .

An independent argument against a high-power jet can be put forward by considering knot-A. In the kinematic model of Biretta (1993), knot-A represents a strong transverse shock in the flow where the jet decelerates from  $\Gamma \sim 3$  to  $\Gamma \sim 1.5$ . A substantial part of the kinetic luminosity would then be converted to other forms at the shock. Thus, the fact that we only see  $\sim 2 \times 10^{42} \text{ erg s}^{-1}$  radiated at this knot suggests that the jet does not possess a kinetic luminosity that is orders of magnitude above this value. Note that the fact that the flow remains collimated after knot-A suggests that the kinetic energy is *not* transformed purely into internal energy of the jet material. Even in the more physically plausible oblique shock models of Bicknell & Begelman (1996), a jet with a high kinetic luminosity ( $L_K \gtrsim 10^{44} \text{ erg s}^{-1}$ ) would be expected to radiate more than is observed. Thus, a high jet power necessarily entails problems in understanding the properties of knot-A.

Of course, the above arguments cannot rule out the possibility that the jet has undergone a recent dramatic increase in kinetic luminosity. Such an increase could lead to a powerful VLBI core whilst still keeping the total (average) energetics of the system at the level observed. If the jet has undergone a dramatic increase in power, one might expect to observe the effects of this within the inner jet (i.e. between the core and knot-A, where we have independent arguments for a  $L_K \sim 10^{43} \text{ erg s}^{-1}$  jet.) However, the inner jet is fairly featureless, displaying only the relatively weak knots D, E, and F. Furthermore, there is no precedent for the core of M87 to undergo large amplitude (i.e. order of magnitude) variability. Thus, to postulate a transient increase in jet power would be an ad-hoc way to bypass the energetic constraints presented below.

## 4.2 $L_K$ and the physical jet parameters

To relate the limits on  $L_K$  to physical parameters of the jet, we assume the jet to be uniform in the sense that the density and velocity are constant across a cross-section of the jet at a given distance,  $Z$ , along the jet. If positive charge carriers have mass  $m_+$  per unit electron charge, the total jet kinetic luminosity is given by

$$L_K = \pi r(Z)^2 \beta (\Gamma - 1) \Gamma n (m_e \langle \gamma \rangle + m_+ \langle \gamma_+ \rangle) c^3, \quad (10)$$

where  $r(Z)$  is the physical radius of the jet a distance  $Z$  away from its origin. The inclusion of the  $\langle \gamma \rangle$  and  $\langle \gamma_+ \rangle$  terms allow for energy that is advected within the bulk flow for the electron and positive charge carrier populations respectively.

From the above equation,  $n$  can be expressed in terms of quantities for which we have observational constraints and evaluated for the case of an electron-proton jet ( $m_+ = 1836m_e$ ) and an electron-positron jet ( $m_+ = m_e$ ) at the 5 GHz self-absorption point. We assume that  $L_{43} = 1$ ,  $\Gamma = 3$  and  $\langle \gamma \rangle = 10$  (corresponding to the  $\gamma_{\min} \approx 1$  case). Relaxation of these assumptions are discussed in the next section. For the electron-positron jet ( $m_+ = m_e$ ,  $\langle \gamma_+ \rangle = \langle \gamma \rangle \approx 10$ ) the result is  $n \approx 1.3 \times 10^2 \text{ cm}^{-3}$ . For the electron-proton jet, the proton population will be essentially cold unless the average energy per electron is comparable to or greater than the proton rest mass (i.e.  $\langle \gamma \rangle \gtrsim 2000$ ). In this case ( $m_+ = 1836m_e$ ,  $\langle \gamma_+ \rangle \approx 1$ ) we deduce  $n \approx 1.4 \text{ cm}^{-3}$ . These results are shown as horizontal lines on Fig. 1.

Examination of Fig. 1 strongly suggests the jet to be dominated by an electron-positron plasma rather than an electron-proton plasma. The 22 GHz VLBI data and 100 GHz VLBI data lead to a similar conclusion. This is the main result of the present paper.

The only way for the above constraints to be compatible with an electron-proton jet is if the relativistic electron population has a low-energy cutoff at  $\gamma_{\min} m_e c^2$  with  $\gamma \gg 1$ . Using either the 5 GHz or 22 GHz constraints requires  $\gamma_{\min} > 10$ . The 100 GHz constraints require  $\gamma_{\min} > 100$  (assuming the core is still self-absorbed at this frequency). Physically, increasing  $\gamma_{\min}$  allows the normalization of the relativistic particle distribution,  $N_0$ , to increase whilst holding the density,  $n$ , fixed. Since the synchrotron self-absorption constraints depend only on  $N_0$ , varying  $\gamma_{\min}$  allows the synchrotron constraints to decouple from the kinetic energy constraints. In particular, line B on Fig. 1 will move downwards as  $\gamma_{\min}$  increases such as to keep the combination  $n \gamma_{\min} B^2$  constant. Observational and theoretical constraints on  $\gamma_{\min}$  will be considered in the next Section. It will be seen that the range of parameter space available for an electron-positron jet is relatively small and not easily justifiable on physical grounds. Furthermore, the electron-proton solution is vulnerable to any future tightening of these observational constraints.

## 5 DISCUSSION

The above constraints argue for an electron-positron jet as opposed to an electron-proton jet. In this section we examine the robustness and self-consistency of this result. We then discuss some astrophysical implications.

### 5.1 The dimension of the self-absorbed core

We have taken the angular size of the resolved core, as determined from 5 GHz VLBI, to represent the diameter of the jet at the point where it just becomes self-absorbed. More precisely, this should be considered an *upper limit* to the jet dimension. The VLBI core dimension might plausibly represent the (projected) length of the entire self-absorbed jet. The effect of this uncertainty on our constraints is simply addressed by re-calculating Fig. 1 for a smaller jet diameter. Suppose the physical jet diameter was a factor of 2 smaller than that inferred from VLBI observations. The synchrotron surface brightness constraint, eqn. (6), becomes tighter (i.e. the upper limit on  $B$  reduces) by a factor of 4 (since the surface brightness is twice that observed). The optical depth constraint also become tighter by a factor of 2. The net effect is to raise the (synchrotron) lower limit on  $n\gamma_{\min}$  by a factor of 32. By contrast, the values of  $n$  derived from the kinetic luminosity will only be raised by a factor of 4. Thus, the net effect is to tighten the argument against an electron-proton jet.

If the jet in the core is, in fact, significantly narrower than the VLBI resolution then even the electron-positron solution violates the synchrotron constraints. This is an argument against such a narrow jet.

### 5.2 The effect of a high velocity jet-core

It is physically plausible that the jet starts as a high Lorentz factor beam ( $\Gamma \gg 10$ ) and subsequently decelerates via dissipative processes or entrainment of surrounding material (Begelman, Rees & Sikora 1994; Sikora, Begelman & Rees 1994). The VLBI jet may then possess a high Lorentz factor core surrounded by a slower sheath ( $\Gamma \sim \text{few}$ ). The emission from the core would be largely beamed out of our line of sight and thus would be swamped by emission from the slower sheath. Our above synchrotron constraints would apply only to the outer sheath since it would dominate the observed radio emission. However, since the kinetic energy constraints are based on the large scale energetics of the system, postulating the presence of an unseen rapid core reduces the inferred kinetic luminosity of the outer sheath and thus makes the case against an electron-proton jet stronger.

### 5.3 Synchrotron self-Compton radiation and observational limits on $\gamma_{\min}$

#### 5.3.1 Synchrotron self-Compton radiation

The production of high-energy synchrotron self-Compton (SSC) radiation is an unavoidable consequence of the synchrotron process. We must check that our jet models are consistent with the constraint that the SSC radiation does not violate the observed X-ray limits on the core flux. We can also use this constraint to place observational limits on  $\gamma_{\min}$ .

The SSC X-ray flux density,  $F_X$  from the self-absorbed region (size  $r$ ) is given by G92 as

$$F_X = \frac{2\alpha F_m n \sigma_T r \gamma_{\min}^{2\alpha}}{t(\alpha)} \left(\frac{\nu_m}{\nu_X}\right)^\alpha \ln\left(\frac{\nu_b}{\nu_m}\right), \quad (11)$$

where  $\nu_X$  is the X-ray frequency,  $\nu_b$  is the high-energy cutoff

in the synchrotron spectrum and  $t(\alpha)$  is a function tabulated in G92. We typically assume that  $\nu_b$  lies somewhere between optical and X-ray frequencies. Evaluating this flux density at 1 keV for parameters relevant to the 5 GHz self absorbed region gives

$$F_X \approx 3.0 \times 10^{-11} n \gamma_{\min} \ln(\nu_b/\nu_m) \text{ Jy}. \quad (12)$$

where

$$\ln(\nu_b/\nu_m) \sim 10 \quad (13)$$

for physically plausible values of  $\nu_b$ . For consistency, this must be less than the observed X-ray core flux density of  $\sim 3.5 \times 10^{-7} \text{ Jy}$  (BSH). We note that using the result of Section 3.3 we can rewrite this as a function of the VLBI core flux density and the magnetic field  $B$  only. This gives a lower limit on the magnetic field of  $B \gtrsim 0.01 \text{ G}$ .

For pair jets, we have shown from our kinetic luminosity arguments that  $n \approx 10^2 \text{ cm}^{-3}$ . The production of synchrotron self-Compton radiation is then consistent with observations provided  $\gamma_{\min} \lesssim 10$  (in which case, a substantial fraction of the observed X-rays will originate from the SSC process). For an electron-proton jet ( $n \approx 1 \text{ cm}^{-3}$ ) the corresponding limit is  $\gamma_{\min} \lesssim 10^3$ .

#### 5.3.2 SSC limits and $\gamma_{\min}$

The SSC limits give  $B \gtrsim 0.01 \text{ G}$ . Thus, an electron energy distribution that cuts off at  $\gamma_{\min}$  will produce a low-energy cutoff in the synchrotron spectrum at frequency  $\nu_c \sim \gamma_{\min}^2 (B/\text{G}) \text{ MHz}$ . Observationally,  $\nu_c < 1 \text{ GHz}$  leading to the condition that  $\gamma_{\min} < 100$ . Thus, if  $10 < \gamma_{\min} < 100$ , the electron-proton jet is consistent with our 5 GHz and 22 GHz constraints. If the core emission is still dominated by self-absorbed radiation at 100 GHz, the corresponding VLBI constraints are incompatible with an electron-proton jet since compatibility would demand  $\gamma_{\min} \sim 100$  which would lead to an unobserved low-frequency cut off at  $\nu_c \sim 100 \text{ GHz}$  (note that the SSC limit on the magnetic field at the 100 GHz self-absorption location is  $B \gtrsim 10 \text{ G}$ ).

### 5.4 Theoretical issues related to $\gamma_{\min}$

In the absence of further observational limits on  $\gamma_{\min}$ , we briefly discuss some related theoretical issues.

Let us suppose that the relativistic electron population at the 5 GHz self-absorbed point did, in fact, possess a low-energy cutoff corresponding to  $\gamma_{\min} \sim 10\text{--}100$ . Such an energy distribution cannot be a relic of the conditions imposed near the base of the jet: synchrotron and inverse Compton losses would have cooled a significant number of these electron to energies below  $10m_e c^2$ . Thus, some in-situ physical mechanism must be maintaining this low-energy cutoff (i.e. by either reheating the electrons/positrons or injecting fresh high-energy pairs).

One mechanism that has been proposed for injecting high-energy pairs into a jet is that of high-energy hadronic (primarily proton-proton, hereafter p-p) collisions (Falcke & Biermann 1995; Biermann, Strom & Falcke 1995). Such collisions produce both charged and neutral pions. The charged pions then decay into electrons or positrons, corresponding to the  $\pi^-$  and  $\pi^+$  cases respectively, with an initially high

energy ( $\gamma \sim 100$ ) due to the large rest mass of the pions. However, the p-p interaction cross section is approximately  $\sigma_{pp} \approx \sigma_T/10$  (and decreases as  $\gamma$  increases). Thus, the optical depth to p-p collisions at the location where our VLBI constraints are applied is  $\lesssim 10^{-8}$  (where we have used the fact that the number density of protons is constrained to be  $n_p \lesssim 1 \text{ cm}^{-3}$  by the kinetic luminosity constraint). We conclude that this mechanism is not relevant in this case. In fact, it would only be relevant at the base of very powerful (and compact) jets. We note that hadronic processes may be of importance in compact plasmas near the centre of the accretion flow (Sikora et al. 1987; Begelman, Rudak & Sikora 1990). In the absence of any other mechanism that inject high-energy electrons, any low-energy cutoff seen at the 5 GHz self-absorption point is not likely to be due to such injection.

Various heating mechanisms that could lead to  $\gamma_{\min} > 1$  have been discussed by G92. The most likely heating mechanism is that due to synchrotron self-absorption (the so-called ‘synchrotron boiler’; Ghisellini, Guilbert & Svensson 1988). For the region under consideration here, electrons radiating at the self-absorption frequency (5 GHz) have  $\gamma \sim 100$ . If only synchrotron processes were important (i.e. the plasma is magnetically dominated), the electron energy distribution below this would possess a quasi-thermal component (due to the efficient exchange of energy between the relativistic electrons). The effective low-energy cutoff would then lie somewhere below  $\gamma_{\min} \sim 100$ . However, if inverse Compton losses are important (as is probably the case for jets on the VLBI scale), the effective low-energy cutoff will be much reduced and, indeed, synchrotron heating can become irrelevant. A detailed treatment of this phenomenon is beyond the scope of this paper.

### 5.5 Annihilation of the pairs

The cross-section for annihilation of cold (i.e. non-relativistic) pairs is given by  $\sigma_a = (3/8)\sigma_T$  where  $\sigma_T$  is the Thomson cross-section. [As the pairs become relativistic, the cross-section declines in a manner analogous to the Klein-Nishina decline of the Thomson cross-section.] In the comoving frame, the rate of annihilation of cold pairs is then

$$\dot{n} = \frac{3}{8}c\sigma_T n^2, \quad (14)$$

leading to an annihilation timescale of

$$t_{\text{ann}} = \frac{8}{3c\sigma_T n}. \quad (15)$$

In the outer, low-density parts of the jet this timescale is long and annihilation is not an important process. However, in the higher densities found near the jet core the annihilation rate increases. It is instructive to estimate the distance from the nucleus at which the annihilation timescale,  $t_{\text{ann}}$  equals the flow timescale  $t_{\text{flow}} = Z/\Gamma c$  where  $Z$  is the distance from the core. If the jet has a constant opening angle and constant velocity so that the density falls off as  $n \propto Z^{-2}$ , equating  $t_{\text{ann}}$  and  $t_{\text{flow}}$  gives the *annihilation radius*

$$Z_{\text{ann}} = \frac{3\sigma_T n_0 Z_0^2}{8\Gamma}, \quad (16)$$

where  $n_0$  is the particle density at a distance  $Z_0$  along the jet. Our (cold-jet) kinetic luminosity constraints give

$nr^2 = 4 \times 10^{36} \text{ cm}^{-1}$ . If we assume a half opening angle of  $\gtrsim 0.1$  rad (such as to agree with the opening angle on larger scales) then  $Z \lesssim 10r$ . Together with  $\Gamma = 3$ , this evaluates to give  $Z = 3 \lesssim 10^{13} \text{ cm}$ . This is to be compared with the Schwarzschild radius of  $R_s \approx 1 \times 10^{15} \text{ cm}$  ( $M = 3 \times 10^9 M_\odot$  assumed). Thus it is feasible for the jet to have originated from a pair plasma formed at the centre of the accretion flow.

### 5.6 The FR-I/FR-II dichotomy

Celotti & Fabian (1993) utilized SSC constraints on a sample of radio galaxies and radio-loud quasars (dominated by FR-II type objects) and argued for either an electron-positron jet with  $\gamma_{\min} \sim 1$  or an electron-proton jet with a  $\gamma_{\min} \sim 100$ . For these powerful sources, it was found that the annihilation radius lies well outside the region occupied by any compact pair plasma associated with the inner accretion flow. Thus it is not possible to have the pair jet flowing freely from the immediate vicinity of the black hole. This argument was used to favour the electron-proton case. However, we have presented arguments for an electron-positron jet in M87 (a classical FR-I source). These results suggest one of two possibilities:

a) FR-I and FR-II may possess jets of an intrinsically different nature, at least by the time the jet has propagated to VLBI scales: i.e. FR-I sources may possess electron-positron VLBI jets whereas FR-II sources may possess VLBI electron-proton jets. The morphological differences between FR-I/FR-II sources may reflect this underlying difference in the jet (for example, via the ease of collimation). However, it is difficult to envisage the physical processes leading to such a dichotomy and how they could be related to the source power.

b) The annihilation radius constraint does not apply and both classes of sources possess electron-positron jets with  $\gamma_{\min} \sim 1$ . In this case, the jet would have to propagate from the vicinity black hole out to at least the annihilation radius in some other form such as a Poynting flux dominated flow. Beyond the annihilation radius, electromagnetic cascades can lead to copious pair production within the Poynting flux dominated flow.

## 6 CONCLUSIONS AND DEFINITIVE OBSERVATIONS

The M87 jet has the best determined geometry and kinematics of any extragalactic jet in the sky. M87 is also one of the very few galaxies in which the mass of the central black hole ( $2.4 \pm 0.7 \times 10^9 M_\odot$ ) is well constrained (by HST observations). This makes M87 an obvious system in which to study the physical properties of extragalactic jets.

We have utilized the standard theory of synchrotron self-absorbed cores in order to constrain the magnetic field,  $B$ , and the relativistic (proper) particle density,  $n$ , of the jet. The 5 GHz data implies  $n\gamma_{\min} \gtrsim 10 \text{ cm}^{-3}$ . For this jet to carry the kinetic luminosity inferred from global energetic arguments, the density is either  $n \sim 1 \text{ cm}^{-3}$  (electron-proton jet) or  $n \sim 10^2 \text{ cm}^{-3}$  (electron-positron jet). We cite this as evidence for an electron-positron dominated jet rather than an electron-proton dominated jet. An electron-proton

jet with  $10 < \gamma_{\min} < 100$  is consistent with the present (conservative) constraints but is extremely vulnerable to further tightening of the VLBI limits. If the core seen in 100 GHz VLBI data is self-absorbed, the electron-proton jet is ruled out. Some theoretical arguments are also presented detailing the problems of the high- $\gamma_{\min}$  scenario.

To make further observational progress, the self-absorbed core has to be identified and resolved. This requires high-resolution multi-frequency VLBI observations. The sub-arcsec X-ray imaging capability of *AXAF* will separate the core X-ray emission from other components (e.g. inner knot emission) and thus allow stricter limits to be placed on the SSC radiation of the self-absorbed core. Such data, together with arguments similar to those presented here, should allow the matter content of this archetypal extragalactic jet to be unambiguously determined.

## ACKNOWLEDGEMENTS

CSR thanks PPARC for support. ACF, AC and MJR thank the Royal Society for support. We are grateful to Ralph Spencer for his useful comments on the interpretation of the VLBI data.

## REFERENCES

- Bääth L. B. et al., 1992, *A&A*, 257, 31  
 Begelman M. C., Rees M. J., Sikora M., 1994, *ApJ*, 429, L57  
 Begelman M. C., Rudak B., Sikora M., 1990, *ApJ*, 362, 38  
 Bicknell G. V., Begelman M. C., 1996, *ApJ*, in press  
 Biermann P. L., Strom R. G., Falcke H., 1995, *A&A*, 302, 429  
 Biretta J. A., 1993, in *Astrophysical Jets*, p. 263, eds. Burgarella D., Livio M., O'Dea C. P., Cambridge University Press, Cambridge (B93)  
 Biretta J. A., Stern C. P., Harris D. E., 1991, *AJ*, 101, 1632 (BSH)  
 Biretta J. A., Zhou F., Owen F. N., 1995, *ApJ*, 447, 582 (BZO)  
 Blandford R. D., Königl A., 1979, *ApJ*, 232, 34  
 Blandford R. D., Payne D. G., 1982, *MNRAS*, 199, 883  
 Celotti A., Fabian A. C., 1993, *MNRAS*, 264, 228  
 Curtis H. D., 1918, *Pub. Lick Obs.*, 13, 31  
 Fabian A. C., Hu E. M., Cowie L. L., Grindlay J., 1981, *ApJ*, 248, 47  
 Falcke H., Biermann P. L., 1995, *A&A*, 293, 665  
 Fanaroff B. L., Riley J. M., 1974, *MNRAS*, 167, 31P  
 Ford H. C. et al. 1995, *ApJ*, 1994, 435, L27  
 Ford H. C., Butcher H., 1979, *ApJS*, 41, 147  
 Ghisellini G., Celotti A., George I. M., Fabian A. C., 1992, *MNRAS*, 258, 776 (G92)  
 Ghisellini G., Guilbert P. W., Svensson R., 1988, *ApJ*, 334, L5  
 Ghisellini G., Padovani P., Celotti A., Maraschi L., 1993, *ApJ*, 407, 65  
 Harms R. J. et al., 1994, *ApJ*, 435, L35  
 Hines D. C., Owen F. N., Eilek J. A., 1989, *ApJ*, 347, 317  
 Jones D. W., O'Dell S. L., Stein W. A., 1974, *ApJ*, 188, 353  
 Junor W., Biretta J. A., 1995, *AJ*, 109, 500  
 Lynden-Bell D., 1996, *MNRAS*, 279, 389  
 Meisenheimer K., Röser H. -J., Schlötelburg M., 1996, *AA*, 307, 61  
 Owen F. N., Hardee P. E., Bignell R. C., 1980, *ApJ*, 239, L11  
 Pauliny-Toth I. I. K., Preuss E., Witzel A., Graham D., Kellerman K. I., Ronnang B., 1981, *AJ*, 86, 371  
 Reid M. J., Biretta J. A., Junor W., Muxlow T. W. B., Spencer R. E., 1989, *ApJ*, 336, 112  
 Rybicki G. B., Lightman A. P., 1979, *Radiative Processes in Astrophysics*, Wiley  
 Sikora M., Begelman M. C., Rees M. J., 1994, *ApJ*, 421, 153  
 Sikora M., Kirk J. G., Begelman M. C., Schneider P., 1987, *ApJ*, 320, L81  
 Sparks W. B., Ford H. C., Kinney A. L., 1993, *ApJ*, 413, 531  
 Spencer R. E., Junor W., 1986, *Nat.*, 321, 753  
 Tonry J. L., 1991, *ApJ*, 373, L1  
 Turland B. D., 1975, *MNRAS*, 170, 281